

case of silicon, the lowest concentration for which signs of impurity band conduction of the type discussed in part II have been observed is about  $10^{17}/\text{cm}^3$ . This is not far below the concentration listed in the last column of Table I, and the germanium results suggest that it will not be difficult to account for this.

## ACKNOWLEDGMENTS

The author gratefully acknowledges many helpful suggestions by Dr. C. Herring, especially on thermoelectric power. Thanks are also due Dr. J. Bardeen for a stimulating discussion, and Mr. G. D. O'Neill for assistance with the manuscript.

PHYSICAL REVIEW

VOLUME 103, NUMBER 1

JULY 1, 1956

## Galvanomagnetic Theory for Electrons in Germanium and Silicon: Magnetoresistance in the High-Field Saturation Limit\*

LOUIS GOLD AND LAURA M. ROTH†

*Lincoln Laboratory, Massachusetts Institute of Technology, Lexington, Massachusetts*

(Received December 23, 1955)

For constant scattering time  $\tau$  and ellipsoidal energy surfaces, the Boltzmann transport equation reduces to a phenomenological equation of motion for electrons from which a conductivity tensor is derived. The calculations for germanium and silicon differ in the orientation of the ellipsoids. The resistivity tensor is evaluated in the saturation limit, and explicit expressions for the angular dependence of the magnetoresistance are elaborated for certain high-symmetry combinations. The theoretical findings are in qualitative agreement with experiment, thus providing confirmation of the 4- or 8-ellipsoid [111] and the 3- or 6-ellipsoid [100] models of the energy surfaces in  $n$  germanium and  $n$  silicon, respectively. Essential agreement with energy-dependent  $\tau$  theory is also established.

## INTRODUCTION

INDEPENDENT reports by Abeles and Meiboom<sup>1</sup> and by Shibuya<sup>2</sup> have demonstrated that the galvanomagnetic behavior of  $n$  germanium is successfully accounted for by the application of Boltzmann transport theory using the model of eight ellipsoidal energy surfaces located along the [111] axis in the Brillouin zone. Their analyses were formulated in terms of an energy-dependent scattering time  $\tau$  which, in particular, represented lattice scattering.

This paper describes a different approach to the problem which was a natural outgrowth of the theoretical interpretation of the cyclotron resonance experiments of Lax, Zeiger, and Dexter<sup>3</sup> in which a constant  $\tau$  was found adequate. It was thought that a constant- $\tau$  theory might adequately describe the observations of Pearson and Suhl,<sup>4</sup> although such a restrictive assumption is not truly justified over all temperatures. The advantage of this approach is that the Boltzmann theory reduces to a relatively simple phenomenological description. We also by-pass the difficulties involved in carrying through a precise treatment of the scattering processes. It is known that there are uncertainties in the temperature variation of the mass ratio  $K$ , the

validity of neglecting intervalley and interband scattering,<sup>5</sup> and the anisotropy of  $\tau$ . Thus, one may not be much worse off in working with a constant  $\tau$ .

In this light, our theory, while not generally physically realistic, has the virtue of being the simplest possible approach. This is not to say that it is entirely rid of cumbersome algebra; but at least the results can be more clearly expressed and explicitly evaluated. While we will initially follow a course which is applicable over all ranges of magnetic field, we will specialize to the high-field saturation limit when taking the inverse of the conductivity tensor, and leave the more complicated intermediate field case for a separate report. This permits us to concentrate on the magnetoresistance in this paper, since for  $H \rightarrow \infty$  the Hall coefficient  $R_H$  is simply  $(nqc)^{-1}$ .

### PHENOMENOLOGICAL CALCULATION OF THE EFFECTIVE CONDUCTIVITY TENSOR FOR COMBINATIONS OF ELLIPSOIDAL ENERGY SURFACES

Use of the constant  $\tau$  in the Boltzmann transport equation leads to the phenomenological equation of motion first proposed by Shockley<sup>6</sup>:

$$[(\nu + j\omega)\mathbf{m} + q\mathbf{B} \times] \mathbf{v} = q\mathbf{E}, \quad \nu = 1/\tau. \quad (1)$$

The relation describes the forced, damped oscillation of an electron in a single ellipsoidal energy surface characterized by the mass tensor  $\mathbf{m}$ , which is given in

\* The research reported in this document was supported jointly by the Army, Navy, and Air Force under contract with Massachusetts Institute of Technology.

† Now at Harvard University, Cambridge, Massachusetts.

<sup>1</sup> B. Abeles and S. Meiboom, *Phys. Rev.* **95**, 31 (1954).

<sup>2</sup> M. Shibuya, *Phys. Rev.* **95**, 1385 (1954).

<sup>3</sup> Lax, Zeiger, and Dexter, *Physica* **20**, 818 (1954).

<sup>4</sup> G. L. Pearson and H. Suhl, *Phys. Rev.* **83**, 768 (1951).

<sup>5</sup> C. Herring, *Bell System Tech. J.* **34**, 237 (1955).

<sup>6</sup> W. Shockley, *Phys. Rev.* **90**, 491 (1953).

the ellipsoidal system by

$$\mathbf{m}' = \begin{bmatrix} m_1 & 0 & 0 \\ 0 & m_2 & 0 \\ 0 & 0 & m_2 \end{bmatrix}. \quad (2)$$

The impressed electric field is periodic,  $\mathbf{E}(t) = \mathbf{E}e^{j\omega t}$ ; the dc case simply has  $\omega = 0$ .

The conductivity tensor  $\sigma$  for the single surface can be derived by introducing the unit tensor  $\mathfrak{I}$  so that Eq. (1) may be written as

$$[(m/m_2) + \mathbf{b} \times \mathfrak{I}] \mathbf{v} = \frac{q}{(\nu + j\omega)m_2} \mathbf{E}, \quad (3)$$

where

$$\mathbf{b} = \frac{q\mathbf{B}}{m_2(\nu + j\omega)}, \quad (4)$$

$$\mathbf{b} \times \mathfrak{I} = \begin{bmatrix} 0 & -b_3 & b_2 \\ b_3 & 0 & -b_1 \\ -b_2 & b_1 & 0 \end{bmatrix}. \quad (5)$$

Thus, from  $\mathbf{J} = nq\mathbf{v}$  it follows that

$$\frac{\sigma}{\sigma^*} = \frac{3K}{2K+1} \left[ \frac{\mathbf{m}}{m_2} + \mathbf{b} \times \mathfrak{I} \right]^{-1}, \quad K = m_1/m_2, \quad (6)$$

where

$$\sigma^* = \frac{nq^2}{\bar{m}^*(\nu + j\omega)} \quad (7)$$

is the ordinary conductivity, and  $\bar{m}^*$  is the average effective mass given by

$$3/\bar{m}^* = (2/m_2) + (1/m_1). \quad (8)$$

We must now refer the separate conductivity contributions from the various ellipsoids to a common reference frame so that they may be summed.

#### A. 4 or 8 [111] Ellipsoids for Germanium

The ellipsoidal axes for the four sets of energy surfaces are given in the Appendix, along with the matrices  $\mathfrak{S}^i$  which transform from these axes to the cubic axes. With  $\mathbf{b}$  specified in relation to the cubic axes, and the mass tensors given by

$$\mathbf{m}_i = (\mathfrak{S}^i)^{-1} \mathbf{m}' \cdot \mathfrak{S}^i,$$

where  $\mathbf{m}'$  is given by Eq. (2), we average Eq. (6) over the four sets of ellipsoids. The result can be put in the form

$$\sigma/\sigma^* = \begin{bmatrix} a_1 & c_3 + d_3 & c_2 - d_2 \\ c_3 - d_3 & a_2 & c_1 + d_1 \\ c_2 + d_2 & c_1 - d_1 & a_3 \end{bmatrix}, \quad (9)$$

with

$$\begin{aligned} a_1 &= \left[ \frac{1}{4} \sum_i \frac{1}{\Delta_i} \right] \left( 1 + \frac{3}{2K+1} b_1^2 \right), \\ c_1 &= \left[ \frac{1}{4} \sum_i \frac{1}{\Delta_i} \right] \frac{3}{2K+1} b_2 b_3 - \left[ \frac{1}{4} \sum_i \frac{S_1^i}{\Delta_i} \right] \frac{K-1}{2K+1}, \\ d_1 &= \left[ \frac{1}{4} \sum_i \frac{1}{\Delta_i} \right] \frac{K+2}{2K+1} b_1 + \frac{K-1}{2K+1} \left[ \frac{1}{4} \sum_i \frac{S_2^i b_3 + S_3^i b_2}{\Delta_i} \right], \\ \Delta_i &= \frac{1}{K} \det \left[ \frac{\mathbf{m}_i}{m_2} + \mathbf{b} \times \mathfrak{I} \right] = 1 + \frac{1}{K} b^2 + \frac{K-1}{3K} \cdot (S_1^i b_1 + S_2^i b_2 + S_3^i b_3)^2, \end{aligned} \quad (10)$$

the remaining tensor components coming from cyclic permutation of Eq. (10). The  $S_1^i$ , etc., are given in the appendix.

#### B. 3 or 6 [100] Ellipsoids for Silicon

The mass tensor  $\mathbf{m}_1$  for the ellipsoids along the  $k_x$  axis is given by Eq. (2), with  $m_2$  and  $m_3$  given by cyclic permutations. The conductivity tensor is again given by Eq. (9), where now

$$\begin{aligned} a_1 &= \frac{1}{2K+1} \left( \frac{1}{\Delta_1} + \frac{K}{\Delta_2} + \frac{K}{\Delta_3} + \sum_i \frac{1}{\Delta_i} - b_1^2 \right), \\ c_1 &= \sum_i \frac{1}{\Delta_i} b_2 b_3 \frac{1}{2K+1}, \\ d_1 &= \frac{b_1}{2K+1} \left( \frac{K}{\Delta_1} + \frac{1}{\Delta_2} + \frac{1}{\Delta_3} \right), \text{ etc;} \\ \Delta_i &= \frac{1}{K} \det \left[ \frac{\mathbf{m}_i}{m_2} + \mathbf{b} \times \mathfrak{I} \right] = 1 + \frac{1}{K} b^2 + \frac{K-1}{K} b_i^2. \end{aligned} \quad (11)$$

#### SATURATION LIMIT FOR THE RESISTIVITY TENSOR

In passing to the high-field limit, we expand the conductivity tensor in inverse powers of  $H$ , and the following form results:

$$\sigma/\sigma^* \cong A \mathfrak{I} \mathfrak{I} - \frac{1}{b} (\mathbf{D} \times \mathfrak{I}) + \frac{1}{b^2} \mathfrak{C}, \quad (12)$$

where  $A$ ,  $\mathbf{D}$ , and  $\mathfrak{C}$  take on different values for Ge and Si, and  $\mathfrak{I}$  is the unit vector in the direction of the magnetic field. We expand  $\sigma^{-1}$ , treating the last term as small:

$$\begin{aligned} \frac{\rho}{\rho^*} &= \left( \frac{\sigma}{\sigma^*} \right)^{-1} \cong \left( A \mathfrak{I} \mathfrak{I} - \frac{1}{b} \mathbf{D} \times \mathfrak{I} \right)^{-1} \\ &\quad \cdot \left[ 1 - \frac{1}{b^2} \mathfrak{C} \cdot \left( A \mathfrak{I} \mathfrak{I} - \frac{1}{b} \mathbf{D} \times \mathfrak{I} \right)^{-1} \right]. \end{aligned} \quad (13)$$

We find

$$\left(A\mathfrak{g}\mathfrak{g}-\frac{1}{b}\mathbf{D}\times\mathfrak{g}\right)^{-1}=\frac{1}{A(\mathfrak{g}\cdot\mathbf{D})^2}\times[\mathbf{D}\mathbf{D}+Ab(\mathfrak{g}\cdot\mathbf{D})(\mathfrak{g}\times\mathfrak{g})]. \quad (14)$$

If we make use of the fact that for both cases [Eqs. (23) and (25) below],

$$\mathfrak{g}\cdot\mathbf{D}=3K/(2K+1), \quad (15)$$

then Eq. (13) becomes

$$\frac{\rho}{\rho^*}\cong\left(\frac{3K+1}{3K}\right)^2\left[\frac{\mathbf{D}\mathbf{D}}{A}-(\mathfrak{g}\times\mathfrak{g})\cdot\mathfrak{C}\cdot(\mathfrak{g}\times\mathfrak{g})\right]+\left(\frac{3K+1}{3K}\right)b(\mathfrak{g}\times\mathfrak{g}). \quad (16)$$

Note that the last term yields a Hall coefficient  $R_H=1/nqc$ .

Finally, if  $\alpha$  is the unit current vector, we have for the resistance  $\rho$  and the magnetoresistance  $\Delta\rho/\rho^*$ :

$$\frac{\rho}{\rho^*}=1+\frac{\Delta\rho}{\rho^*}=\alpha\cdot\frac{\rho}{\rho^*}\cdot\alpha=\left(\frac{3K+1}{3K}\right)^2\left[\frac{(\alpha\cdot\mathbf{D})^2}{A}+(\mathfrak{g}\times\alpha)\cdot\mathfrak{C}\cdot(\mathfrak{g}\times\alpha)\right]. \quad (17)$$

#### A. Saturation Magnetoresistance $\Delta\rho/\rho^*$ for Germanium

In the tensor  $\mathfrak{C}$ , Eq. (17),

$$\mathfrak{C}=\begin{bmatrix}\bar{a}_1 & \bar{c}_3 & \bar{c}_2 \\ \bar{c}_3 & \bar{a}_2 & \bar{c}_1 \\ \bar{c}_2 & \bar{c}_1 & \bar{a}_3\end{bmatrix}, \quad (18)$$

we have for the components

$$\bar{a}_1=\bar{a}_2=\bar{a}_3=\bar{a}=\frac{1}{4}\sum_i\frac{1}{\Delta_i},$$

$$c_j=-\frac{1}{4}\sum_i\frac{S_j^i}{\Delta_i'}\left(\frac{K-1}{2K+1}\right), \quad j=1, 2, 3. \quad (19)$$

where

$$\Delta_i'=\lim_{b\rightarrow\infty}\Delta_i/b^2=\frac{1}{K}+\frac{K-1}{3K}(S_1^i\beta_1+S_2^i\beta_2+S_3^i\beta_3)^2. \quad (20)$$

Then in the other expressions we have

$$A=\frac{1}{4}\sum_i\frac{1}{\Delta_i'}\left(\frac{3}{2K+1}\right),$$

$$\bar{d}=\frac{1}{4}\sum_i\frac{1}{\Delta_i'}\left(\frac{K+2}{2K+1}\right)\beta_1$$

$$+\frac{1}{4}\left(\frac{K-1}{2K+1}\right)\sum_i\frac{1}{\Delta_i'}(S_2^i\beta_3+S_3^i\beta_2), \quad (21)$$

with  $\bar{d}_2$  and  $\bar{d}_3$  formed from  $\bar{d}_1$  by cyclic permutations.

#### B. Saturation Magnetoresistance for Silicon

Here the components of the tensor  $\mathfrak{C}$  in Eq. (22) are the diagonal elements

$$a_1=\frac{1}{2K+1}\left(\frac{1}{\Delta_1'}+\frac{K}{\Delta_2'}+\frac{K}{\Delta_3'}\right), \text{ etc.}, \quad (22)$$

with  $\bar{c}_1=\bar{c}_2=\bar{c}_3=0$ . The  $\Delta_i'$  are given by

$$\Delta_i'=\lim_{b\rightarrow\infty}\frac{\Delta_i}{b^2}=\frac{1}{K}[1+(K-1)\beta_i^2]. \quad (23)$$

Then, for the remaining quantities,

$$A=\frac{1}{2K+1}\sum_i\frac{1}{\Delta_i'},$$

$$\bar{d}_i=\frac{\beta_i}{2K+1}\left(\frac{K}{\Delta_1'}+\frac{1}{\Delta_2'}+\frac{1}{\Delta_3'}\right), \text{ etc.} \quad (24)$$

#### ANGULAR DEPENDENCE OF $\Delta\rho/\rho$ IN GERMANIUM

The directional effects that have been experimentally observed may be checked with Eq. (17) by consideration of two special cases.

##### A. Special Cases $B_3=0$

The expression for  $\rho/\rho^*$  reduces to

$$\frac{\rho}{\rho^*}=\frac{(2K+1)/9K(K+2)}{(K+2)^2-4(K-1)^2\beta_1^2\beta_2^2}$$

$$\times\{[(K+2)^2-2(K-1)^2\beta_2^2]\alpha_1\beta_1$$

$$+[(K+2)^2-2(K-1)^2\beta_1^2]\alpha_2\beta_2\}^2$$

$$+3(2K+1)(K+2)^2[1-(\alpha_1\beta_1+\alpha_2\beta_2)^2]$$

$$-12(K-1)^2(K+2)\beta_1^2\beta_2^2\alpha_3^2\}. \quad (25)$$

Then for the following particular current directions the angular dependence of the magnetoresistance may be determined.

1.  $\mathbf{J}_{100}$ ,  $\alpha_2=\alpha_3=0$ ,  $\alpha_1=1$ :

$$\frac{\rho}{\rho^*}=\frac{2K+1}{9K(K+2)}$$

$$\times\frac{[(K+2)^2-2(K-1)^2\beta_2^2]^2\beta_1^2+3(2K+1)(K+2)^2\beta_2^2}{(K+2)^2-4(K-1)^2\beta_1^2\beta_2^2}. \quad (26)$$

For numerical evaluation, we employ the cyclotron resonance value of the longitudinal and transverse masses<sup>3</sup>:

$$m_1=1.4 m_0, \quad m_2=0.083 m_0, \quad K=16.8. \quad (27)$$

In Fig. 1(a) the behavior of  $\Delta\rho/\rho$  is depicted as the magnetic vector is rotated in the (001) plane. The expected  $\pi$  symmetry is evidenced and the longitudinal magnetoresistance exceeds the transverse in agreement

with experiment. The expression for the ratio of longitudinal to transverse  $\Delta\rho/\rho^*$  is given by

$$\left(\frac{\Delta\rho}{\rho^*}\right)_L / \left(\frac{\Delta\rho}{\rho^*}\right)_T = \frac{2}{3}(K+2), \quad (28)$$

which is greater than unity for  $K>1$ ; in particular, for  $K=16$  it has a value of 12.

2.  $\mathbf{J}_{110}$ ,  $\alpha_1=\alpha_2=1/\sqrt{2}$ ,  $\alpha_3=0$ :

$$\frac{\rho}{\rho^*} = \frac{2K+1}{18K(K+2)} \frac{[(K+2)^2 - 2(K-1)^2\beta_1\beta_2](\beta_1+\beta_2)^2 + 3(2K+1)(K+2)^2(\beta_1-\beta_2)^2}{(K+2)^2 - 4(K-1)^2\beta_1^2\beta_2^2}. \quad (29)$$

The required  $\pi$  symmetry occurs as shown in Fig. 1(b). Also this arrangement exhibits a transverse magneto-resistance greater than the longitudinal alignment—again in agreement with observation<sup>4</sup>;

$$\left(\frac{\Delta\rho}{\rho^*}\right)_L / \left(\frac{\Delta\rho}{\rho^*}\right)_T = \frac{(K-1)^2}{3K(K+2)}, \quad (30)$$

which is always less than unity for  $K>1$ , and for  $K=16$  is 0.26.

3.  $\mathbf{J}_{001}$ ,  $\alpha_1=\alpha_2=0$ ,  $\alpha_3=1$ :

$$\frac{\rho}{\rho^*} = \frac{2K+1}{3K} \frac{(K+2)(2K+1) - 4(K-1)^2\beta_1^2\beta_2^2}{(K+2)^2 - 4(K-1)^2\beta_1^2\beta_2^2}. \quad (31)$$

This properly shows the  $\pi/2$  symmetry as may be seen from Fig. 1(c), having a maximum value of  $\mathbf{B}_{110}$  with the minimum at the transverse position  $\mathbf{B}_{100}$ .

### B. Special Case $B_1 = B_2$

This corresponds to the magnetic vector in the (110) plane with  $\beta_1=\beta_2=\beta/\sqrt{2}$ . Now Eq. (21) reduces to

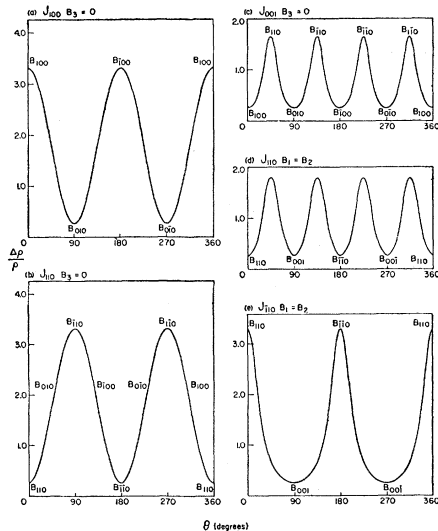


FIG. 1. Variation of  $\Delta\rho/\rho^*$  for the 4- or 8-ellipsoid model of  $n$  Ge in the saturation limit, as the magnetic field is rotated through the angle  $\theta$ . Current directions are as shown, and the cardinal directions for  $\mathbf{B}$  are indicated.

$$\begin{aligned} \frac{\rho}{\rho^*} = & \left(\frac{2K+1}{3K}\right)^2 \left\{ \frac{1}{A} \left[ \frac{(\alpha_1+\alpha_2)}{\sqrt{2}} \bar{d} + \alpha_3 \bar{d}_3 \right]^2 \right. \\ & + \bar{a} \left[ 1 - \left( \frac{(\alpha_1+\alpha_2)}{\sqrt{2}} \beta + \alpha_3 \beta_3 \right)^2 \right] - \bar{c} \beta \beta_3 (\alpha_1 - \alpha_2)^2 \\ & \left. - \bar{c}_3 (\beta \alpha_3 - \sqrt{2} \beta_3 \alpha_3) (\beta \alpha_3 - \sqrt{2} \beta_3 \alpha_1) \right\}, \quad (32) \end{aligned}$$

where

$$\begin{aligned} \bar{a} = & \frac{3K+1}{3} A = \frac{3K}{D} [(K+2)^2 + (K-1)(K+2)\beta^2 \\ & - 4(K-1)^2\beta^2\beta_3^2], \\ \bar{c}_1 = \bar{c}_2 = & \frac{c}{\sqrt{2}} = \frac{3K(K-1)^2}{D(2K+1)} [K+2 - (K-1)\beta^2], \\ \bar{c}_3 = & \frac{3K(K-1)^2}{D(2K+1)} [2K+1 - 5(K-1)\beta_3^2], \\ \bar{d}_1 = \bar{d}_2 = & \frac{\bar{d}}{\sqrt{2}} = \frac{K+1}{2K+1} \bar{a} \beta - \left( \frac{\bar{c}}{\sqrt{2}} \right) \beta_3 - \bar{c}_3 \beta, \\ \bar{d}_3 = & \frac{K+2}{2K+1} \bar{a} \beta_3 - \left( \frac{\bar{c}}{\sqrt{2}} \right) \beta, \\ D = & [K+2 - (K-1)\beta^2] \\ & \times \{ [K+2 + (K-1)\beta^2]^2 - 8(K-1)^2\beta^2\beta_3^2 \}. \quad (33) \end{aligned}$$

Here the special current directions of interest may be introduced:

1.  $\mathbf{J}_{110}$ ,  $\alpha_1=\alpha_2=1/\sqrt{2}$ ,  $\alpha_3=0$ :

$$\frac{\rho}{\rho^*} = \left(\frac{2K+1}{3K}\right)^2 \left[ \frac{\bar{d}}{A} + (\bar{a} - \bar{c}_3)\beta_3^2 \right]. \quad (34)$$

The angular dependence of  $\Delta\rho/\rho$  exhibits  $\pi/2$  symmetry with a maximum at  $\theta=45^\circ$  and equivalent minima at  $\mathbf{B}_{110}$  and  $\mathbf{B}_{001}$ . [See Fig. 1(d).]

2.  $\mathbf{J}_{110}$ ,  $\alpha_1=-\alpha_2=-1/\sqrt{2}$ ,  $\alpha_3=0$ :

$$\frac{\rho}{\rho^*} = \left(\frac{2K+1}{3K}\right)^2 [\bar{a} - 2\bar{c}\beta\beta_3 + \bar{c}_3\beta_3^2]. \quad (35)$$

The behavior of  $\Delta\rho/\rho^*$  may be seen in Fig. 1(e). The  $\pi$  symmetry is characterized by a maximum at  $\mathbf{B}_{110}$  and a minimum at  $\mathbf{B}_{001}$ .

ANGULAR DEPENDENCE OF  $\Delta\rho/\rho^*$  IN SILICON

 A. Special Case  $B_3=0$ 

The expression for  $\rho/\rho^*$  is

$$\frac{\rho}{\rho^*} = \frac{(K+2)(2K+1)}{9K} + \frac{(K-1)^2(2K+1)[2\alpha_1\alpha_2\beta_1\beta_2 - 2(\alpha_1^2\beta_1^2 + \alpha_2^2\beta_2^2) - (K-1)\beta_1^2\beta_2^2(1-\alpha_3^2)]}{9K[2K+1+(K-1)^2\beta_1^2\beta_2^2]}. \quad (36)$$

1.  $J_{100}$ :

$$\frac{\rho}{\rho^*} = \frac{(K+2)(2K+1)}{9K} - \frac{(K-1)^2(2K+1)[2+(K-1)\beta_2^2]\beta_1^2}{9K[2K+1+(K-1)^2\beta_1^2\beta_2^2]}. \quad (37)$$

The over-all behavior of the  $\Delta\rho/\rho^*$  is illustrated in Fig. 2(a) which should be contrasted with the result for germanium contained in Fig. 1; the longitudinal magnetoresistance is zero, in agreement with Herring and Pearson<sup>7</sup> as is the  $\pi$  symmetry. The curve is plotted for the data derived from cyclotron resonance<sup>8</sup>:

$$m_1 = 0.98m_0, \quad m_2 = 0.19m_0, \quad K = 5.2. \quad (38)$$

2.  $J_{001}$ :

For this current direction the magnetoresistance is constant as the magnetic vector is rotated in the orthogonal plane:

$$\frac{\rho}{\rho^*} = \frac{(K+2)(2K+1)}{9K}. \quad (39)$$

3.  $J_{110}$ :

$$\frac{\rho}{\rho^*} = \frac{(K+2)(2K+1)}{9K} - \frac{(K-1)^2(2K+1)[1-\beta_1\beta_2+(K-1)\beta_1^2\beta_2^2]}{9K[2K+1+(K-1)^2\beta_1^2\beta_2^2]}. \quad (40)$$

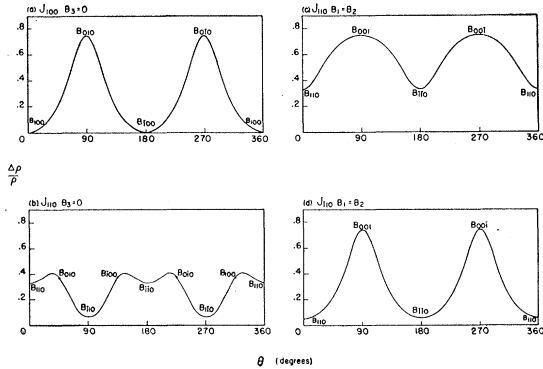


FIG. 2. Variation of  $\Delta\rho/\rho^*$  for the 3- or 6-ellipsoid model of  $n$ -Si in the saturation limit, as the magnetic field is rotated through the angle  $\theta$ . Current directions are as shown, and the cardinal directions for  $\mathbf{B}$  are indicated.

<sup>7</sup> G. L. Pearson and C. Herring, *Physica* **20**, 975 (1954).

<sup>8</sup> R. N. Dexter and B. Lax, *Phys. Rev.* **96**, 233 (1954).

$\Delta\rho/\rho^*$  shows the striking behavior depicted in Fig. 2(b). While  $\pi$  symmetry is manifested, the appearance of an intermediate peak adds an interesting aspect not encountered in the experimental work; unfortunately Herring and Pearson<sup>7</sup> did not study this situation. The maximum occurs at about  $35^\circ$  for  $K \sim 5$  and the upper minimum is at  $\mathbf{B}_{110}$  with the lower one at  $\mathbf{B}_{\bar{1}\bar{1}0}$ .

 B. Special Case  $B_1=B_2$ 

For this case

$$\frac{\rho}{\rho^*} = \frac{(K+2)(2K+1)}{9K} + \frac{(K-1)^2(2K+1)}{9K[2K+1+(K-1)^2\beta^2(1-\frac{3}{4}\beta^2)]} \times \left\{ \left(1 + \frac{K-1}{2}\beta^2\right) \left[ \frac{\alpha_1+\alpha_2}{\sqrt{2}}\alpha_3\beta\beta_3 - \frac{\beta^2}{2} \left(\frac{\alpha_1+\alpha_2}{\sqrt{2}}\right)^2 \right] - \left(\frac{\alpha_1-\alpha_2}{\sqrt{2}}\right)^2 \frac{\beta^2}{2} [(2K+1) - \frac{3}{2}\beta^2(K-1)] - \alpha_3^2\beta_3^2[2+\beta^2(K-1)] \right\}, \quad (41)$$

and we consider the following current directions:

1.  $J_{110}$ :

$$\frac{\rho}{\rho^*} = \frac{(K+2)(2K+1)}{9K} - \frac{(K-1)^2(2K+1)\beta^2(1+K-\frac{1}{2}\beta^2)}{18K[2K+1+(K-1)^2\beta^2(1-\frac{3}{4}\beta^2)]}. \quad (42)$$

$\Delta\rho/\rho^*$  shows the angular dependence of Fig. 2(c). The features of  $\pi$  symmetry, minimum at  $\mathbf{B}_{110}$ , maximum at  $\mathbf{B}_{001}$  are precisely those observed.<sup>7</sup>

2.  $J_{\bar{1}\bar{1}0}$ :

$$\frac{\rho}{\rho^*} = \frac{(K+2)(2K+1)}{9K} - \frac{(K-1)^2(2K+1)\beta^2[2K+1-\frac{3}{2}(K-1)\beta^2]}{18K[2K+1+(K-1)^2\beta^2(1-\frac{3}{4}\beta^2)]}. \quad (43)$$

As Fig. 2(d) shows, this reflects  $\pi$  symmetry with a minimum at  $\mathbf{B}_{110}$  and a maximum at  $\mathbf{B}_{001}$ .

## SUMMARY OF RESULTS

In Table I are summarized the saturation magnetoresistance for high-symmetry longitudinal and trans-

TABLE I. Comparison of our results (G-R) with those of Abeles and Meiboom and Shibuya (A-M-S). The constant  $C=32/9\pi$  for A-M-S and 1 for G-R. The  $K$  values are those taken from cyclotron resonance<sup>a</sup>; these have been somewhat revised.<sup>b</sup>

| $J$ and $B$<br>vectors | 4- or 8-ellipsoid model           |  |      | 3- or 6-ellipsoid model           |   |       |
|------------------------|-----------------------------------|--|------|-----------------------------------|---|-------|
|                        | $\rho/\rho^*=1+(\Delta\rho/\rho)$ | $\Delta\rho/\rho$ for<br>$K=16.9$<br>( $n$ -germanium) |      | $\rho/\rho^*=1+(\Delta\rho/\rho)$ | $\Delta\rho/\rho$ for<br>$K=5.2$<br>( $n$ -silicon) |       |
|                        |                                   | A-M-S  | G-R  |                                   | A-M-S   | G-R   |
| [100]                  | $\frac{(2K+1)(K+2)}{9K}$          | 3.3  | 3.3  | 1                                 | 0   | 0     |
| [100]<br>[001]         | $C\frac{(2K+1)^2}{3K(K+2)}$       | 0.43   | 0.26 | $C\frac{(2K+1)(K+2)}{9K}$         | 0.98  | 0.75  |
| [110]                  | $\frac{(2K+1)^2}{3K(K+2)}$        | 0.26   | 0.26 | $\frac{(2K+1)(K+1)}{K(K+5)}$      | 0.33  | 0.33  |
| [110]<br>[110]         | $C\frac{(2K+1)(K+2)}{9K}$         | 3.9  | 3.3  | $C\frac{(2K+1)(5K+1)}{9K(K+1)}$   | 0.20  | 0.061 |

<sup>a</sup> See reference 5.

<sup>b</sup> Dresselhaus, Kip, and Kittel, Phys. Rev. **98**, 368 (1955).

verse arrangements of the current and magnetic vectors; direct comparison with the Abeles and Meiboom<sup>1</sup> and Shibuya<sup>2</sup> results is also made both for general  $K$  and specifically for  $K=16.9$  in Ge and  $K=5.2$  in Si.

It is evident that the longitudinal magnetoresistance in the saturation limit is identical in the constant and energy-dependent  $\tau$  theories. The transverse values differ by a factor of  $32/9\pi$ , brought in by the  $\mathcal{E}^{-1/2}$   $\tau$ -dependence.<sup>9,10</sup> Unfortunately, the experimental data are not adequate to determine which transverse values are appropriate for germanium. The experimental

<sup>9</sup> For a general energy-dependent  $\tau$  this factor becomes  $\bar{\tau}(1/\tau)$ , where the average is taken over energy as in the conductivity.<sup>10</sup> This can be seen by averaging  $\delta^*$  in Eq. (12) over energy, noting that  $\tau$  appears in  $\sigma^*$  and  $b$ .

<sup>10</sup> W. Shockley, *Electrons and Holes in Semiconductors* (D. Van Nostrand and Company, New York, 1950), p. 276, replacing  $\frac{1}{2}mv^2$  by  $\mathcal{E}$ .

saturation values for silicon have not been reported, so little can be said as yet about the theoretical values.

#### ACKNOWLEDGMENTS

We are greatly indebted to several members of the Lincoln Laboratory who contributed materially to this research. Special thanks are due Benjamin Lax, who encouraged the undertaking and with whom we enjoyed interesting discussions, along with H. J. Zeiger, W. Krag, and W. M. Bullis. We particularly appreciated the capable aid of Miss Clare Glennon, who checked the details of the calculations and performed the numerical computations.

#### APPENDIX. [111] ELLIPSOIDAL AXES

The 4 sets of energy surfaces have the following ellipsoidal axes:

|     | $x'$                    | $y'$              | $z'$              |
|-----|-------------------------|-------------------|-------------------|
| I   | $\bar{1}11$             | $\bar{1}10$       | $\bar{1}\bar{1}2$ |
| II  | $\bar{1}\bar{1}1$       | $\bar{1}\bar{1}0$ | $\bar{1}\bar{1}2$ |
| III | $\bar{1}\bar{1}\bar{1}$ | $\bar{1}\bar{1}0$ | $\bar{1}12$       |
| IV  | $\bar{1}1\bar{1}$       | $110$             | $\bar{1}12$       |

Hence, the transformation matrix referring these to the cubic axes reference frame is

$$\mathcal{S}^i = \begin{bmatrix} S_2^i/\sqrt{3} & S_1^i/\sqrt{3} & 1/\sqrt{3} \\ -S_1^i/\sqrt{2} & S_2^i/\sqrt{2} & 0 \\ -S_2^i/\sqrt{6} & -S_1^i/\sqrt{6} & 2/\sqrt{6} \end{bmatrix}, \quad (\text{A-1})$$

where  $S_1^i$ , etc., take on the following values:

|                       | I | II | III | IV |
|-----------------------|---|----|-----|----|
| $S_1^i$               | 1 | 1  | -1  | -1 |
| $S_2^i$               | 1 | -1 | -1  | 1  |
| $S_3^i = S_1^i S_2^i$ | 1 | -1 | 1   | -1 |